Hindawi
Journal of Computer Networks and Communications
Volume 2022, Article ID 9418392, 19 pages
https://doi.org/10.1155/2022/9418392

Research Article

Performance and Improvement Analysis of the Underwater WSN Using a Diverse Routing Protocol Approach

K. Sathish,[1] C. V. Ravikumar ,[1] Asadi Srinivasulu ,[2] A. Rajesh,[3] and Olutayo Oyeyemi Oyerinde[4]

[1] *Vellore Institute of Technology, Vellore, India*
[2] *Data Science Research Lab, BlueCrest University, Monrovia, Liberia*
[3] *School of Electrical and Electronics Engineering, SASTRA University, Thanjavur, India*
[4] *School of Electrical and Information Engineering, University of the Witwatersrand, Johannesburg 2050, South Africa*

Correspondence should be addressed to C. V. Ravikumar; cvrkvit@gmail.com and Asadi Srinivasulu; head.research@bluecrest.edu.lr

Received 23 August 2022; Revised 30 September 2022; Accepted 28 October 2022; Published 9 November 2022

Academic Editor: Roberto Nardone

The planet Earth is the most water-rich place because oceans cover more than 75% of its land area. Because of the extraordinary activities that occur in the depths, we know very little about oceans. Underwater wireless sensors are tools that can continuously transmit data to one of the source sensors while also monitoring and recording the physical and environmental parameters of their surroundings. An underwater wireless sensor network (UWSN) is the name given to the network created by the collection of these underwater wireless sensors. This particular technology is the most efficient way to analyse performance parameters. A network path is chosen to send traffic by using the routing method, a process that is also known as a protocol. The routing protocols ad-hoc on-demand distance vector (AODV), dynamic source routing (DSR), dynamic manet on demand routing protocol (DYMO), location-aided routing 1 (LAR 1), optimized link state routing (OLSR), source-tree adaptive routing optimum routing approach (STAR-ORA), zone routing protocol (ZRP), and STAR-least overhead routing approach (STAR-LORA) are a few models of routing techniques. By changing the number of nodes in the model and the maximum speed of each node, performance parameters such as average transmission delay, average jitter, percentage of utilisation, and power used in transmit and receive modes are explored. The results obtained using QualNet 7.1 simulator suggest the suitability of routing protocols in the UWSN.

1. Introduction

Although water covers a large portion of our planet, much of it is still unknown [1–4]. Exploration in this region has significantly increased recently. In addition to being endowed with abundant natural resources, it has contributed significantly to the development of ships, oil pipelines, and the military. In environments like oceans, seas, and the like, which contain enormous amount of naturally occurring data, this is the researcher's top priority. By developing a variety of UWSN protocols for the underwater environment, the developers have been able to gather and analyse a significant amount of data to some extent [5–8]. Research in this area is built on the findings of earlier studies, as described in the background information below. The general structure of underwater wireless communication is depicted in Figure 1.

1.1. Routing Protocol Abbreviations.

Ad-hoc on-demand distance vector (AODV)

Zone routing protocol (ZRP)

Dynamic source routing protocol (DSR)

fisheye state routing (FSR)

Dynamic MANET on-demand routing protocol (DYMO)

location-aided routing (LAR)

Figure 1: Typical underwater wireless communication structure.

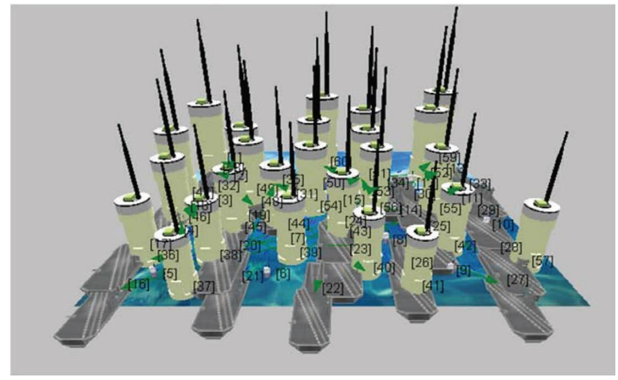

Figure 2: 3D visualization of underwater wireless communication.

Optimized link state routing protocol (OLSR)

Source tree adaptive routing (STAR)

Source tree adaptive routing—optimum routing approach (STAR-ORA)

Source tree adaptive routing—least overhead routing approach (STAR-LORA)

Ad-hoc wireless networks known as wireless sensor networks (WSNs) are used to provide a wireless communication setup, such as for underwater wireless communication [9]. Routing protocols for ad-hoc networks include AODV, DSR, DYMO, LAR1, Bellman–Ford, OLSR, fisheye, STAR-ORA, ZRP, and STAR-LORA, among others [10].

The mobility model shows the movement of nodes as well as how their positions, speeds, and accelerations alter over time. When researching a new network protocol, it is crucial to simulate and assess the protocol's performance. In protocol simulation, the mobility model and the communicating traffic pattern are two crucial variables. Mobility models are used to describe user movement patterns. The state of mobile services is described by the traffic model [11–15]. Figure 2 illustrates a realistic 3D underwater wireless communication scenario with a variety of nodes. The potential challenges posed by the surrounding subsurface environment must be given the attention and consideration they require when thinking about the use of underwater sensor networks [16–18]. The host conditions present numerous difficulties, including three-dimensional topology and continuous node movement. In addition, a lot of underwater applications, like those used for detection or rescue missions, tend to be ad-hoc in nature [19–24].

As depicted in Figure 3, a wireless sensor network (WSN) is made up of spatially dispersed autonomous (self-organized) sensors that monitor environmental or physical conditions such as temperature, sound, vibration, pressure, motion, or pollutants and cooperatively transmit their data through the network to a central location. Modern networks are bidirectional, allowing for the control of sensor activity as well. Military use of wireless sensor networks, such as battlefield surveillance, served as the impetus for their development. Today, these networks are employed in a wide range of commercial and consumer applications, including machine health monitoring, process control, and industrial process monitoring. The WSN is composed of "nodes," which can range in number from a few to thousands and are each connected to one or more sensors [1]. Figure 3 depicts the main parts of a sensor node, which include the following subsystems: a communication (transceiver) subsystem, a computing (processing) subsystem, a sensor subsystem, and a unified power supply system.

1.2. Related Works.

This section of the article examines a previous work from the standpoint of network architecture, as well as the multiple performance measures that support the concept of extending network life.

Bhattacharjya et al. investigated a universal wireless sensor network (UWSN) using a grid topology [25, 26]. This study investigates energy usage across a variety of energy modalities, as well as network performance.

EAVARP, a void-avoidant and energy-conscious routing system, is investigated by Wang et al. for wireless sensor networks [27]. UWSN is impervious to transmission, vacancy, and flooding cycles. UWSN performance parameters include packet delivery ratio, network lifetime, energy utilisation, and transmission latency. In terms of mobility, Alkindi et al. investigated a grid-based routing technique for UWSN [28]. Energy usage, network density, packet delivery ratio, and latency are all discussed.

An optimal, collaborative, and resource-saving strategy is being examined [23]. In order to create a UWSN that consumes less energy, a relay node is chosen. The indices of dead and end-to-end delays, dead packet delivery ratio, and energy usage are investigated. The nodes are organized in a two-dimensional environment with a regular distribution. In the case of the UWSN, both interference and noise are considered. Khan et al. examines interference-free localization routing for ultrawideband sensor networks (UWSNs), with the goal of minimizing the energy hole [23]. It specifies the total number of dropped packets, the total number of dead nodes, a packet received at the sink, the total amount of energy used, and the total number of dropped packets.

The main contribution of the manuscript is highlighted as follows:

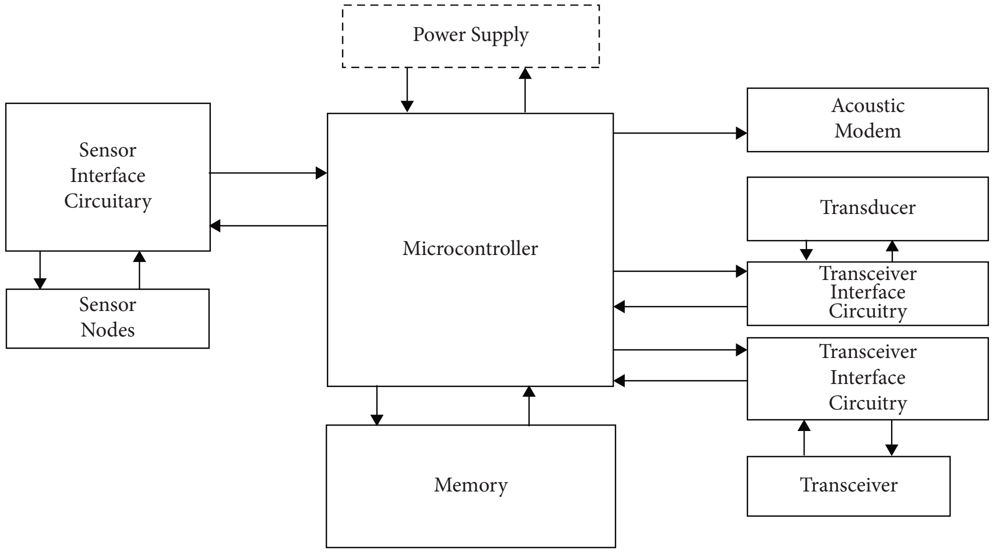

Figure 3: Internal architecture of sensor networks for underwater wireless communication.

(i) To design and implement a source tree adaptive routing—least overhead routing approach (STAR-LORA) protocol for underwater wireless sensors (UWSN) network

(ii) To compare the STAR-LORA routing protocol with standard routing protocols in the literature, namely, AODV, DSR, DYMO, LAR1, Bellman–Ford, OLSR, fisheye, STAR-ORA, and ZRP

(iii) To analyse the energy efficiency of the routing protocol with increasing number of underwater wireless sensor nodes

(iv) To analyse the tradeoff between average transmission delay, average jitter, utilisation rate, and energy in transmit and receive modes

(v) To recommend an appropriate routing protocol based on the targeted performance metric for the underwater wireless sensor network

The remainder of this article is organized as follows. The network scenario is covered in Section 2. The performance parameter is presented in Section 3. We present the findings of our results in Section 4. A comparison of results and discussion are presented in Section 5. In Section 6, we finally conclude.

2. Network Scenario

With CBR as a deployment application, there are accessible existing networks available. In the proposed network, FTP and VBR are taken into account alongside CBR, and the parameters for all three FTP, CBR, and VBR applications are then compared [14, 26, 29–32]. The proposed scenario has a 1500 by 1500 square meter design in the QualNet 7.1 Simulator. The file transfer protocol (FTP), constant bit rate (CBR), and variable bit rate (VBR) applications are connected by both 60 and 120 nodes, of which 15 are node devices, 25 are ship devices, and 20 are sensor devices for 60 nodes and similarly 30 are node devices, 50 are ship devices, and 40 are sensor devices. The simulation lasts for 500 seconds in total. Random way-point mobility with a minimum speed of 1.5 m/sec and a maximum speed of 3 to 10 m/sec is the node mobility model that has been selected. Following AODV as the initial routing protocol are DSR, DYMO, LAR1, Bellman–Ford, OLSR, fisheye, STAR-ORA, ZRP, and STAR-LORA. After finishing the test, the graphs in the simulator were considered. The required performance metrics are thus obtained, including the average transmission delay, average jitter, percentage of utilisation, as well as the energy used in transmit, receive modes. The proposed underwater wireless communication scenario with multiple nodes in X-Y and 3D visualization is shown in Figures 4 and 5, respectively, for 60 nodes. Runtime proposed scenario for the underwater wireless communication with various nodes in both X-Y and 3D visualization is shown in Figures 6 and 7, for 120 nodes [18, 22].

3. Performance Parameters

OPNET, OMNeT, MATLAB, QualNet, and other simulation tools, among others [25, 28, 33–36], commonly take the design of UWSN into account. The proposed network is created in the QualNet simulator using a number of user-friendly UWSN design parameters. The performance indicators for the UWSN network in various applications are listed as shown in Figure 8.

Energy consumption: The energy used by nodes to send data from their point of origin to their point of destination.

Average transmission delay: Average transmission delay is the amount of time it takes for an information to successfully travel from its source to its destination [37].

Average jitter: This is the time difference between individual packets as a result of route changes or network

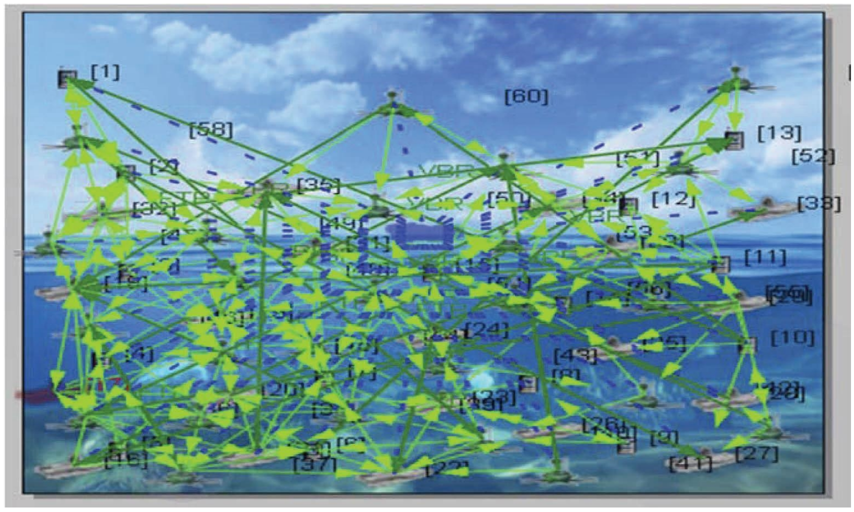

Figure 4: Proposed scenario of underwater wireless communication in X-Y visualization.

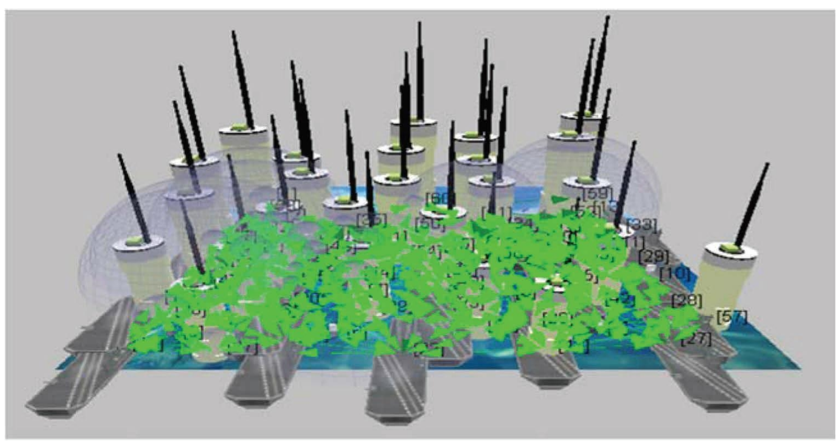

Figure 5: Proposed scenario of underwater wireless communication in 3D visualization.

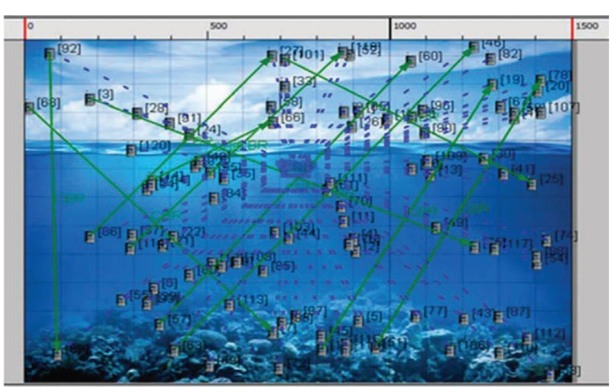

Figure 6: Runtime proposed underwater wireless communication with 120 nodes in X-Y visualization.

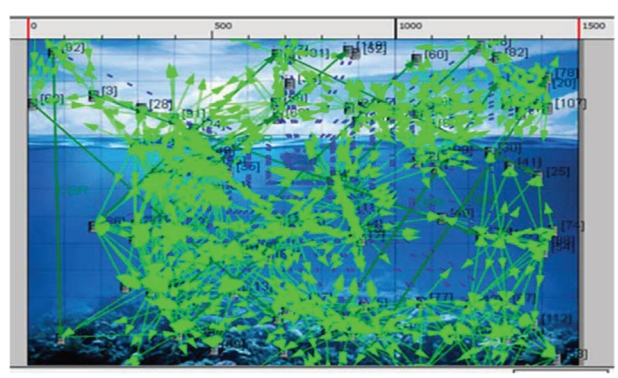

Figure 7: Runtime proposed underwater wireless communication with 120 nodes in *3D* visualization.

congestion. A routing protocol should be lower to function more efficiently. A network's congestion, routing modifications, or timing drift can all increase jitter by delaying the transmission of individual packets [38].

Percentage of utilisation: The proportion of packets that are successfully transferred from the transmitting node to the receiving node is known as the throughput of a communication channel [39].

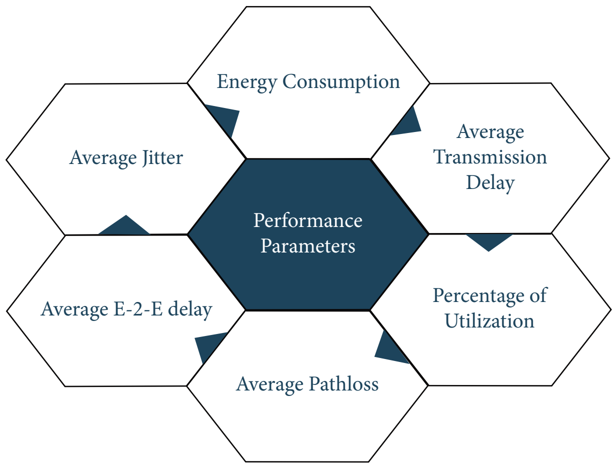

FIGURE 8: Performance parameters of the UWSN.

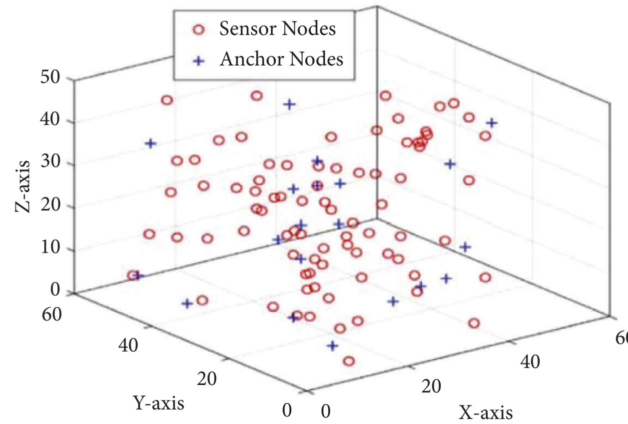

FIGURE 9: Deployment of sensor nodes in 3D for the proposed underwater wireless sensor network.

4. Results and Discussion

In this section, the deployment of sensor nodes in 3D for the proposed UWSN network scenario with sensor nodes and anchor nodes is shown in Figure 9. We have considered the data packet size as 50–100 bytes, transmission energy = 48 dB, propagation speed = $3 \times 10\hat{8}$ m/s, random waypoint mobility with 10 m/s, bit rate = 1 Mbps, transmission range = 50 m, and depth of nodes = 20 m (Max) [40, 41].

In addition, the investigational results for various routing protocols including AODV, DSR, DYMO, LAR1, Bellman–Ford, OLSR, fisheye, STAR-ORA, ZRP, and STAR-LORA with FTP, CBR, and VBR applications are observed for transmit and receive mode power consumption as displayed in Figures 10(a) and 11(t) for both 60 and 120 nodes. As seen from Figures 10(a)–10(t) and Figures 11(a)–11(t) for both 60 and 120 nodes, more power consumption in transmit and receive mode is observed in Bellman–Ford, OLSR, and LAR1 routing protocols. The STAR-ORA, ZRP, and STAR-LORA routing protocols display relatively less power consumption due to the hybrid routing features of these protocols in UWSN scenario.

The findings from measuring the proposed UWSN network's performance parameters in FTP, CBR, and VBR applications for the deployment of 60 and 120 nodes, respectively, are given. The UWSN network's performance metrics for FTP, CBR, and VBR applications are as follows.

4.1. *Energy (mWh) Consumed in Transmit Mode by AODV, DSR, DYMO, LAR1, Bellman–Ford, OLSR, Fisheye, STAR-ORA, ZRP, and STAR-LORA Routing Protocols.*

The energy consumption in transmit mode routing protocols of AODV, DSR, DYMO, LAR1, Bellman–Ford, OLSR, fisheye, STAR-ORA, ZRP, and STAR-LORA with FTP, CBR, and VBR applications for 60 and 120 nodes are displayed in Figures 12 and 13, respectively. As shown in Tables 1 and 2, the minimum transmit energy required by the DSR, DYMO, LAR1, Bellman–Ford, OLSR, fisheye, STAR-ORA, ZRP, and STAR-LORA routing protocols to transmit data at their maximum size in the proposed UWSN is 83.4 percent. Utilizing as little transmit energy as possible is the aim of UWSN. It is impossible for other routing protocols to match AODV's speed and dependability.

4.2. *Energy (mWh) Consumed in Receive Mode by AODV, DSR, DYMO, LAR1, Bellman–Ford, OLSR, Fisheye, STAR-ORA, ZRP, and STAR-LORA Routing Protocols.*

The routing protocols AODV, DSR, DYMO, LAR1, Bellman–Ford, OLSR, fisheye, STAR-ORA, ZRP, and STAR-LORA are compared in Figures 14 and 15 for the amount of received energy they use with FTP, CBR, and VBR applications for 60 and 120 nodes, respectively. The AODV routing protocol uses 76.4 percent less receive energy in CBR application than the other routing protocols shown in Tables 1 and 2, including DSR, DYMO, LAR1, Bellman–Ford, OLSR, fisheye, STAR-ORA, ZRP, and STAR-LORA. When dealing with larger packet sizes than other routing protocols, the AODV routing protocol uses significantly less receive energy than those other routing protocols. When receiving data, UWSN should use the least amount of energy possible. Performance-wise, the AODV routing protocol outperforms other routing protocols.

4.3. *Average Transmission Delay (μsec) by AODV, DSR, DYMO, LAR1, Bellman–Ford, OLSR, Fisheye, STAR-ORA, ZRP, and STAR-LORA Routing Protocols.*

The average transmission delay of AODV, DSR, DYMO, LAR1, Bellman–Ford, OLSR, fisheye, STAR-ORA, ZRP, and STAR-LORA protocol for 60 and 120 nodes, respectively, are displayed in Figures 16 and 17. As shown in Tables 1 and 2, the AODV routing protocol produces an average delay in the CBR application that is 88.6% less than that of other routing protocols.

4.4. *Percentage of Utilization by AODV, DSR, DYMO, LAR1, Bellman–Ford, OLSR, Fisheye, STAR-ORA, ZRP, and STAR-LORA Routing Protocols.*

Tables 1 and 2 demonstrate that the fisheye routing protocol outperformed the competition in terms of percentage of utilisation for the CBR application

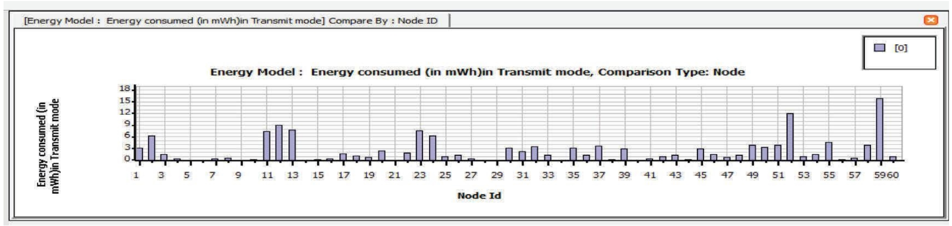

(a)

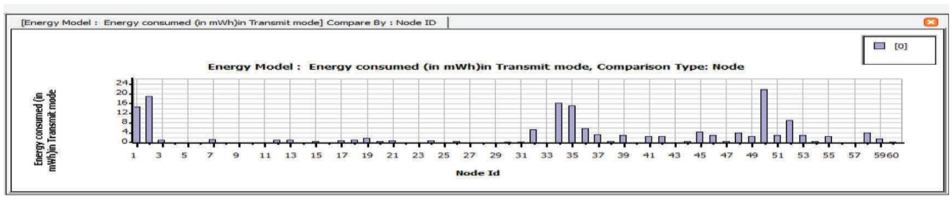

(b)

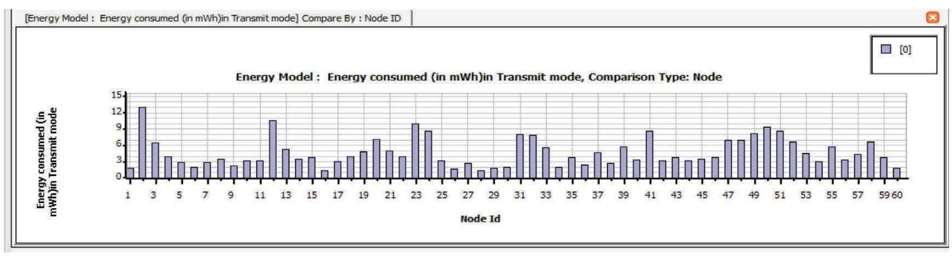

(c)

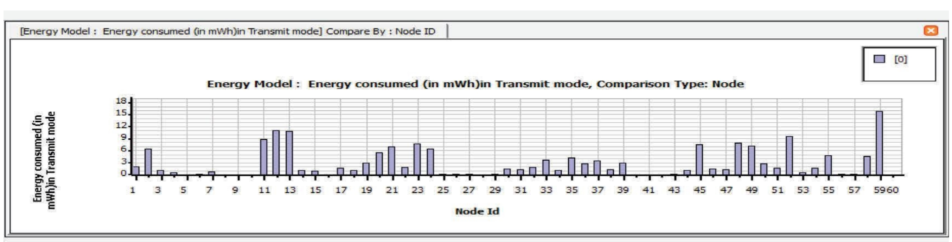

(d)

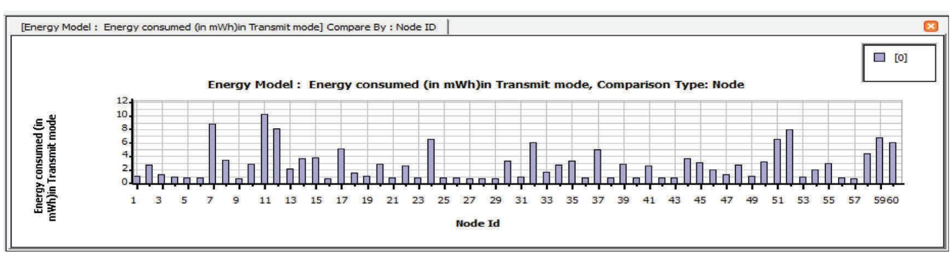

(e)

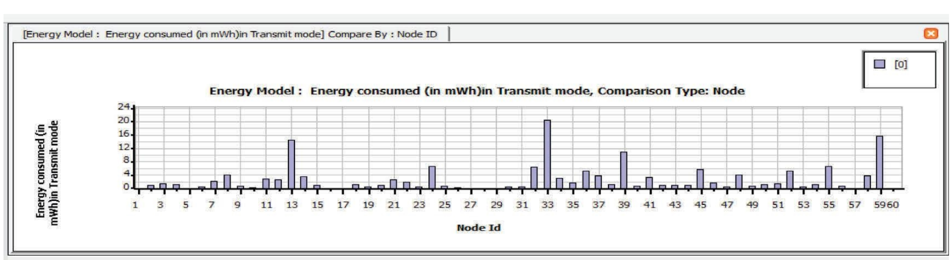

(f)

Figure 10: Continued.

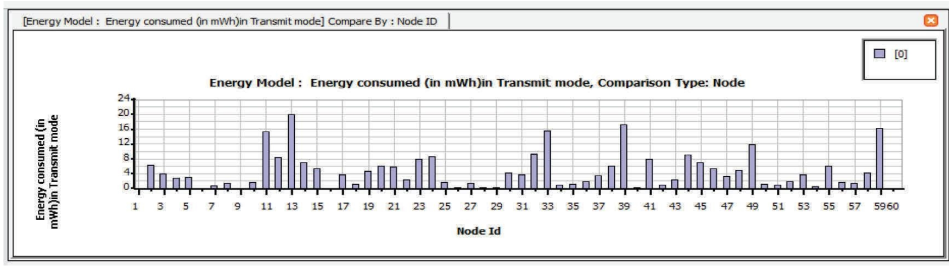

(g)

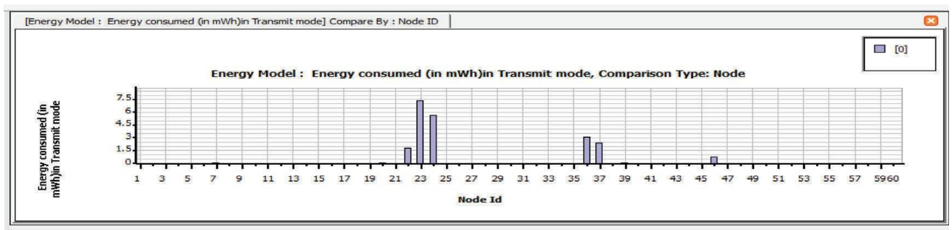

(h)

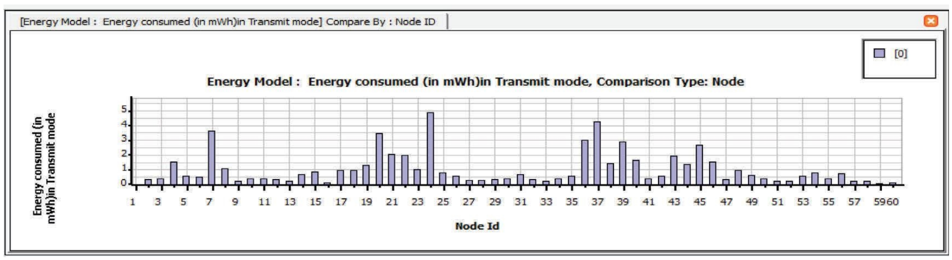

(i)

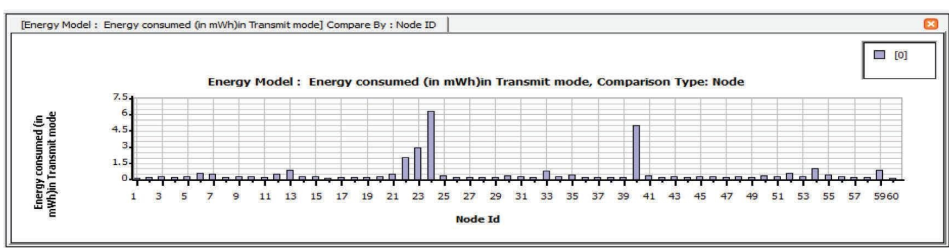

(j)

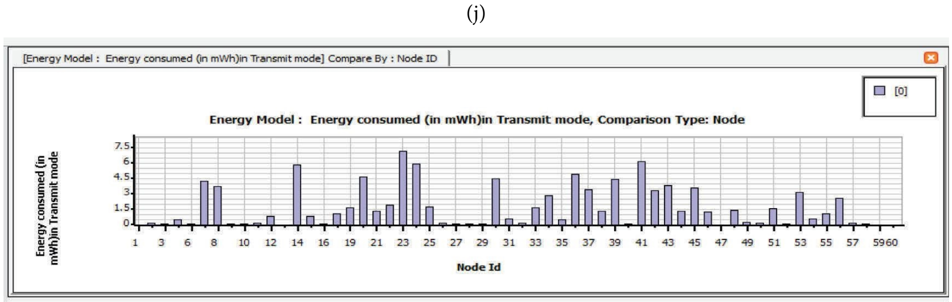

(k)

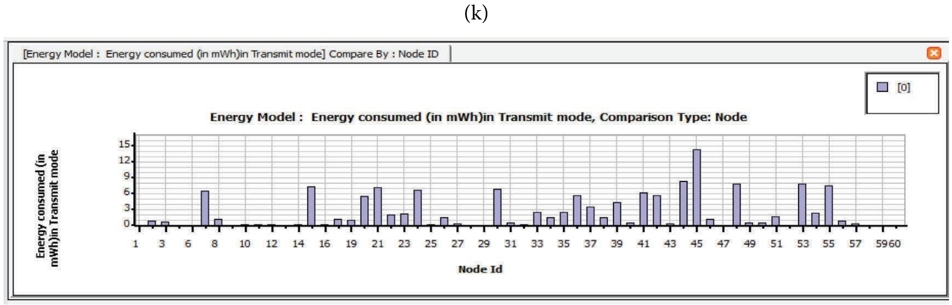

(l)

Figure 10: Continued.

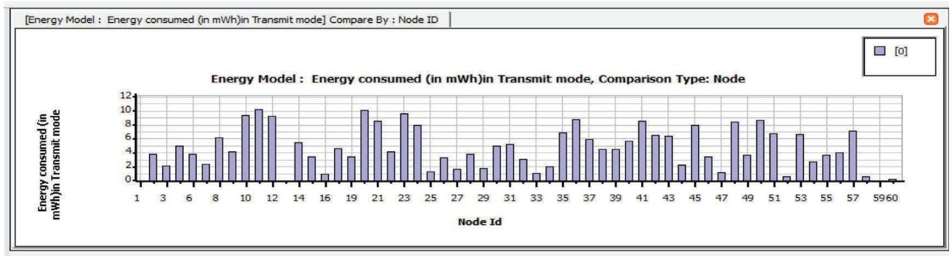

(m)

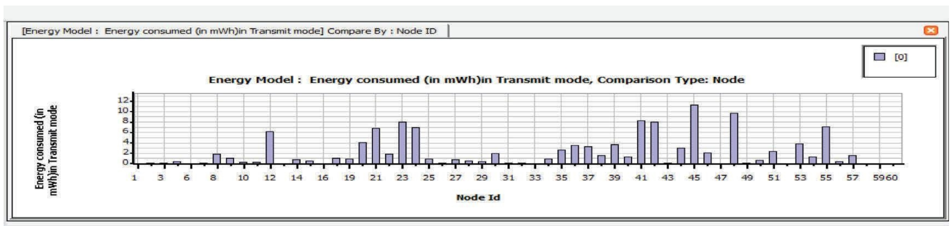

(n)

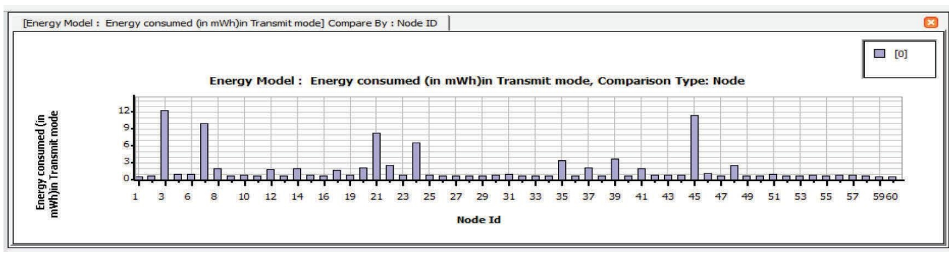

(o)

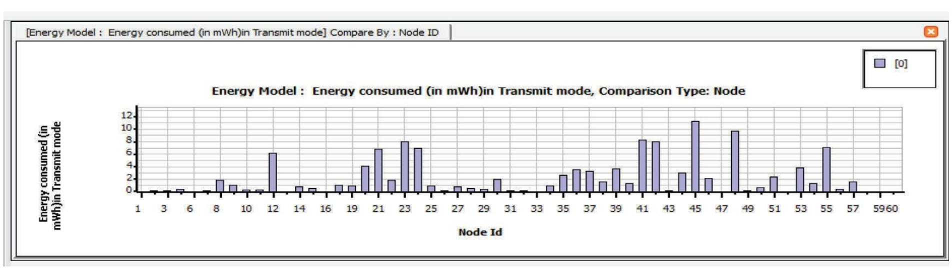

(p)

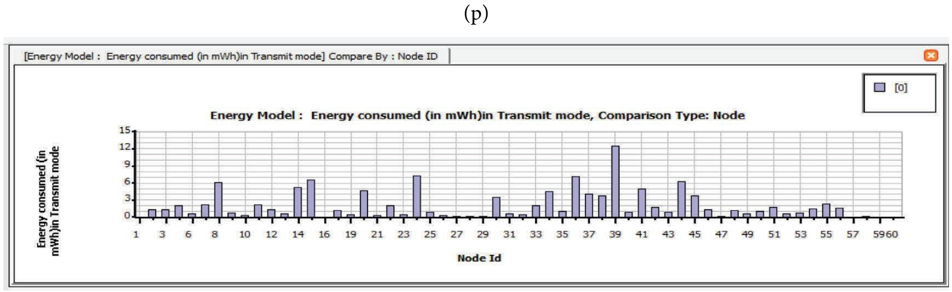

(q)

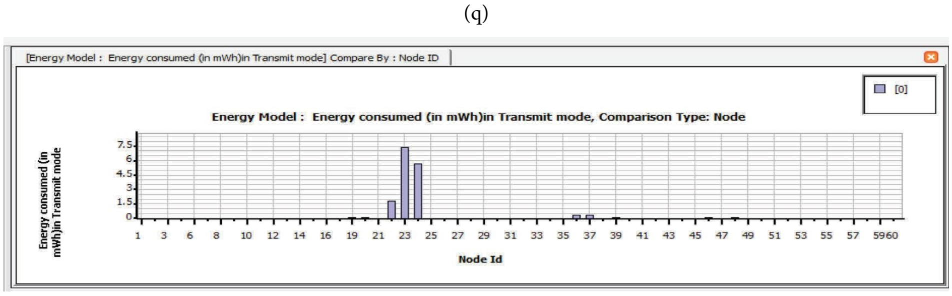

(r)

Figure 10: Continued.

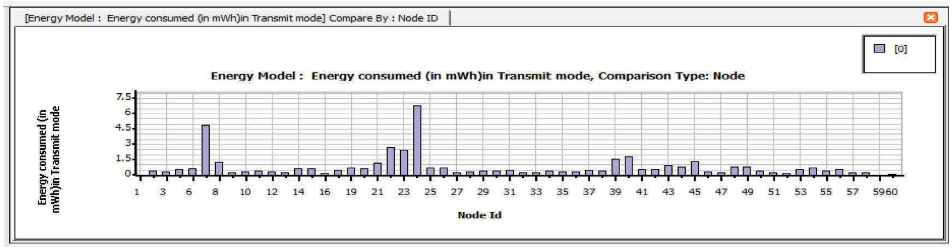

(s)

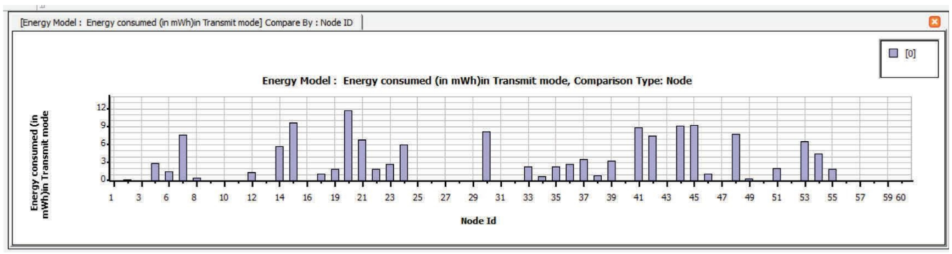

(t)

Figure 10: (a) Transmit mode power consumption (mWh) of AODV for 60 nodes. (b) Transmit mode power consumption (mWh) of DSR for 60 nodes. (c) Transmit mode power consumption (mWh) of DYMO for 60 nodes. (d) Transmit mode power consumption (mWh) of LAR1 for 60 nodes. (e) Transmit mode power consumption (mWh) of OLSR for 60 nodes. (f) Transmit mode power consumption (mWh) of Bellman–Ford for 60 nodes. (g) Transmit mode power consumption (mWh) of Fisheye for 60 nodes. (h) Transmit mode power consumption (mWh) of STAR-LORA for 60 nodes. (i) Transmit mode power consumption (mWh) of ZRP for 60 nodes. (j) Transmit mode power consumption (mWh) of STAR-ORA for 60 nodes. (k) Transmit mode power consumption (mWh) of AODV for 120 nodes. (l) Transmit mode power consumption (mWh) of DSR for 120 nodes. (m) Transmit mode power consumption (mWh) of DYMO for 120 nodes. (n) Transmit mode power consumption (mWh) of LAR1 for 120 nodes. (o) transmit mode power consumption (mWh) of OLSR for 120 nodes. (p) Transmit mode power consumption (mWh) of Bellman–Ford for 120 nodes. (q) Transmit mode power consumption (mWh) of fisheye for 120 nodes. (r) Transmit mode power consumption (mWh) of STAR-ORA for 120 nodes. (s) Transmit mode power consumption (mWh) of ZRP for 120 nodes. (t) Transmit mode power consumption (mWh) of STAR-LORA for 120 nodes.

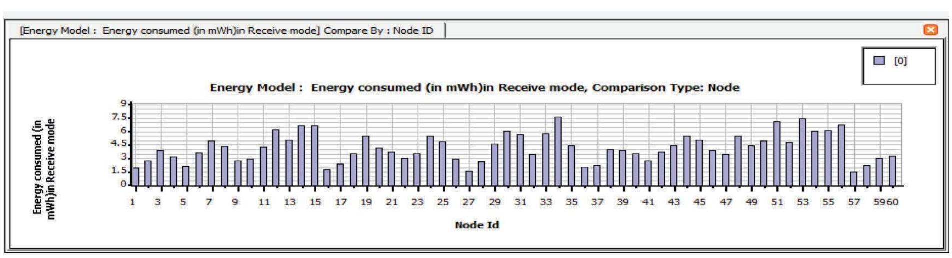

(a)

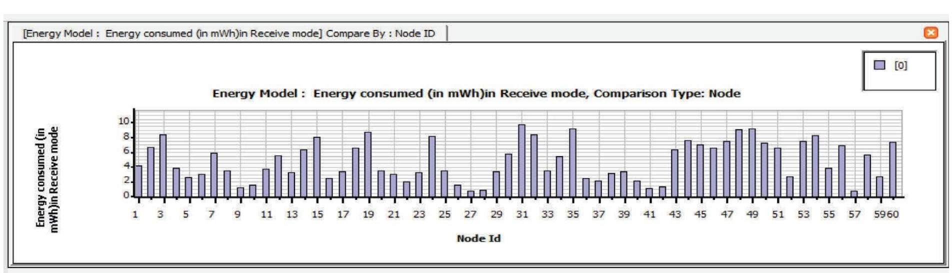

(b)

Figure 11: Continued.

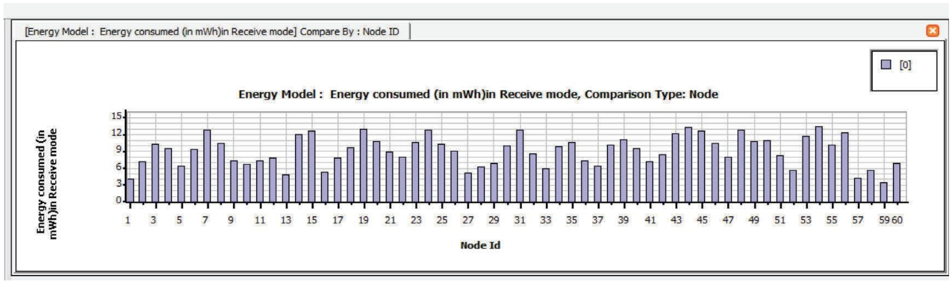

(c)

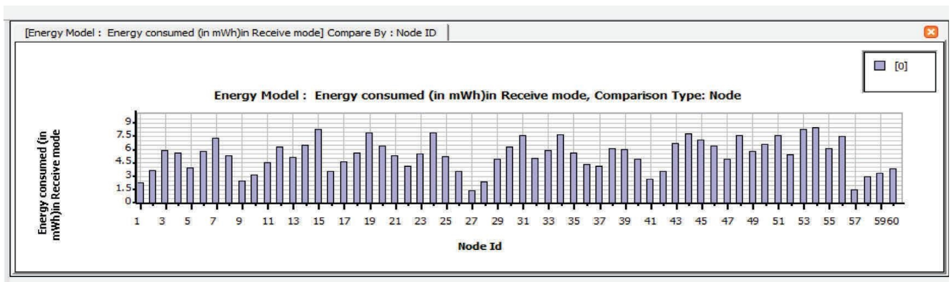

(d)

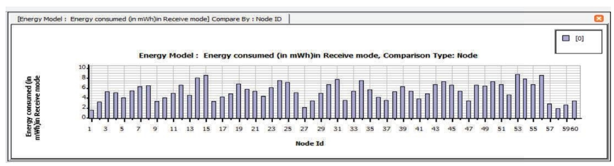

(e)

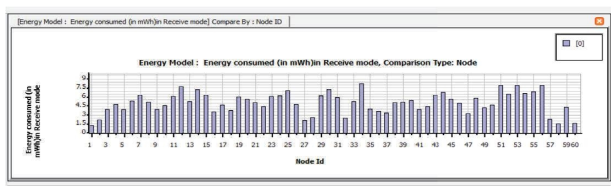

(f)

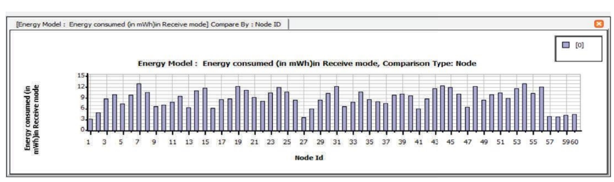

(g)

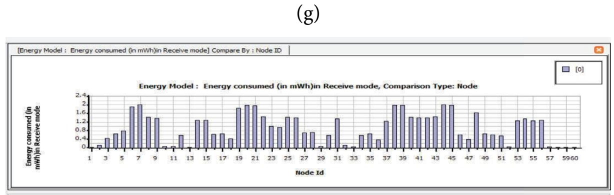

(h)

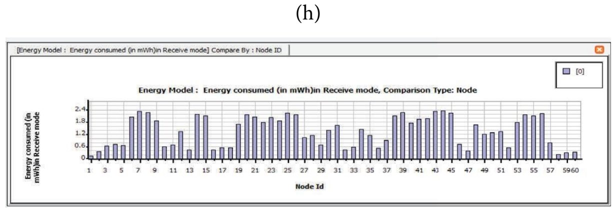

(i)

Figure 11: Continued.

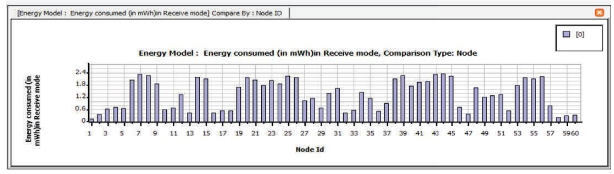

(j)

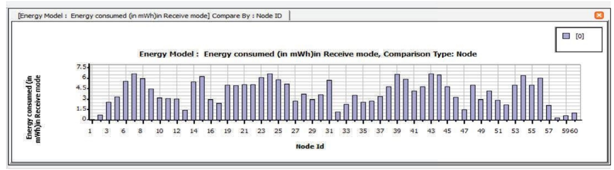

(k)

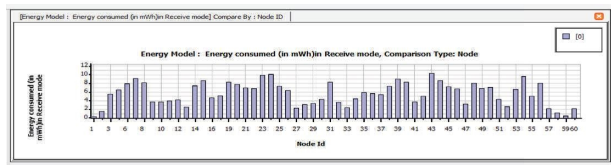

(l)

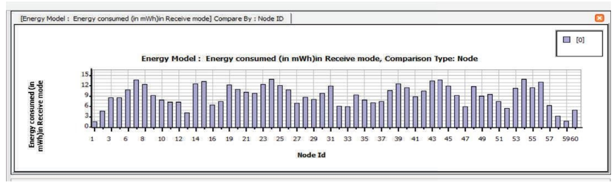

(m)

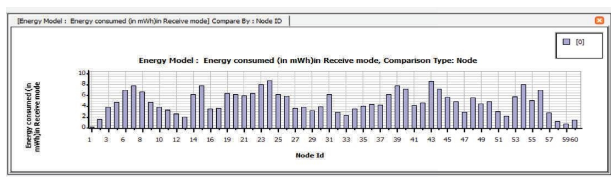

(n)

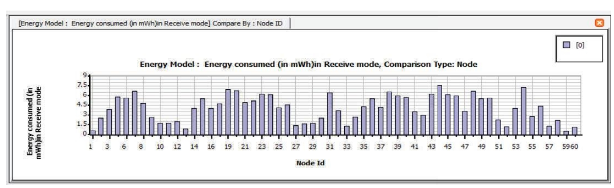

(o)

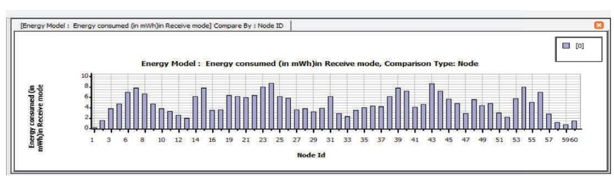

(p)

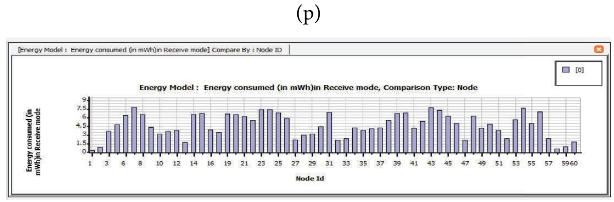

(q)

Figure 11: Continued.

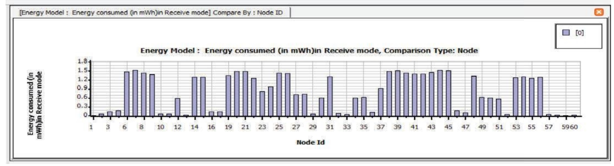

(r)

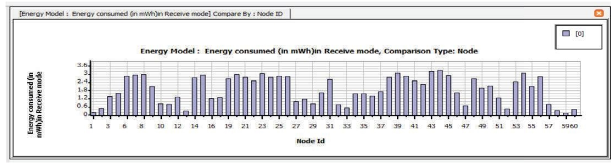

(s)

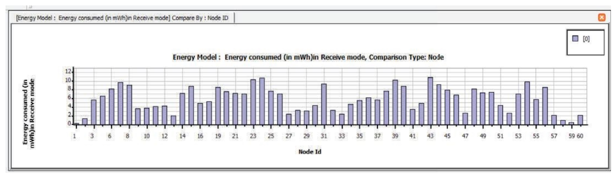

(t)

Figure 11: (a) Receive mode power consumption (mWh) of AODV for 60 nodes. (b) Receive mode power consumption (mWh) of DSR for 60 nodes. (c) Receive mode power consumption (mWh) of DYMO for 60 nodes. (d) Receive mode power consumption (mWh) of LAR1 for 60 nodes. (e) Receive mode power consumption (mWh) of OLSR for 60 nodes. (f) Receive mode power consumption (mWh) of Bellman–Ford for 60 nodes. (g) Receive mode power consumption (mWh) of fisheye for 60 nodes. (h) Receive mode power consumption (mWh) of STAR-LORA for 60 nodes. (i) Receive mode power consumption (mWh) of ZRP for 60 nodes. (j) Receive mode power consumption (mWh) of STAR-ORA for 60 nodes. (k) Receive mode power consumption (mWh) of AODV for 120 nodes. (l) Receive mode power consumption (mWh) of DSR for 120 nodes. (m) Receive mode power consumption (mWh) of DYMO for 120 nodes. (n) Receive mode power consumption (mWh) of LAR1 for 120 nodes. (o) Receive mode power consumption (mWh) of OLSR for 120 nodes. (p) Receive mode power consumption (mWh) of Bellman–Ford for 120 nodes. (q) Receive mode power consumption (mWh) of fisheye for 120 nodes. (r) Receive mode power consumption (mWh) of STAR-ORA for 120 nodes. (s) Receive mode power consumption (mWh) of ZRP for 120 nodes. (t) Receive mode power consumption (mWh) of STAR-LORA for 120 nodes.

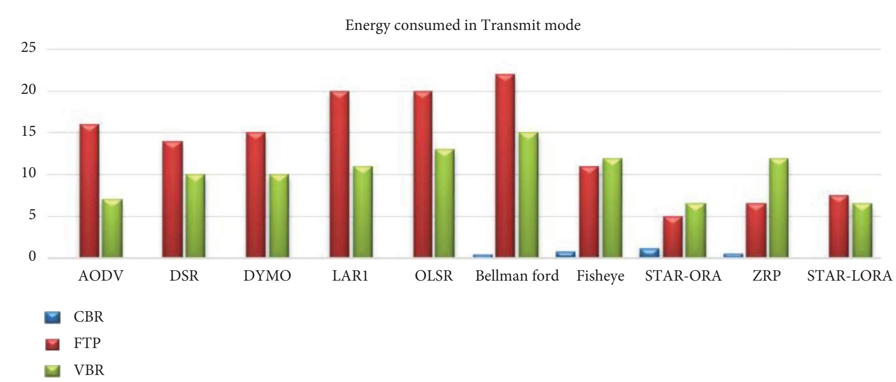

Figure 12: Transmit mode energy consumption of all routing protocols for 60 nodes.

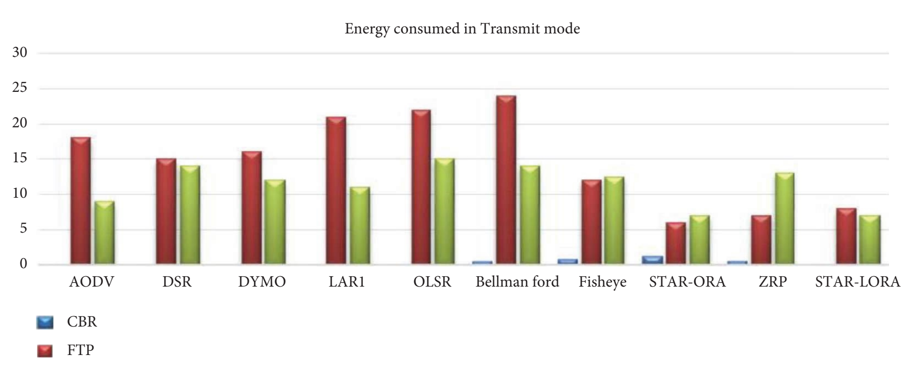

Figure 13: Transmit mode energy consumption of all routing protocols for 120 nodes.

Table 1: Comparison of all routing protocols for 60 nodes.

Parameters	*OLSR*			*DSR*			*AODV*			*LAR1*			*DYMO*			*ZRP*			*STAR-LORA*			*STAR-ORA*			*Fisheye*			*Bellman–Ford*		
	CBR	FTP	VBR	CBR	FTP	VBR	CBR	FTP	VBR	CBR	FTP	VBR	CBR	FTP	VBR	CBR	FTP	VBR	CBR	FTP	VBR	CBR	FTP	VBR	CBR	FTP	VBR	CBR	FTP	VBR
Average transmission delay (μsec)	**28**	**49**	**39**	**23**	**42**	**36**	**18**	**27**	**35**	**27**	**49**	**43**	**31**	**55**	**41**	**28**	**38**	**48**	**35**	**46**	**54**	**30**	**38**	**44**	**25**	**46**	**48**	**33**	**31**	**44**
Receive power consumption (mWh)	**0.2**	**14**	**7.5**	**0.2**	**15**	**13**	**0.2**	**8**	**6.5**	**0.1**	**14**	**8.5**	**0.1**	**8**	**8**	**0.7**	**2.5**	**10**	**0.1**	**2**	**3.5**	**0.5**	**4.5**	**1.5**	**1.2**	**9**	**7.5**	**0.3**	**10**	**10**
Transmit power consumption (mWh)	**0.1**	**20**	**13**	**0.1**	**14**	**10**	**0.1**	**16**	**7**	**0.1**	**20**	**11**	**0.1**	**15**	**10**	**0.6**	**6.5**	**12**	**0.1**	**7.5**	**6.5**	**1.2**	**5**	**6.5**	**0.8**	**11**	**12**	**0.5**	**22**	**15**
Percentage of utilization	**0.7**	**0.9**	**0.8**	**0.7**	**0.7**	**0.3**	**0.3**	**0.2**	**0.1**	**0.6**	**0.2**	**0.2**	**0.6**	**0.6**	**0.2**	**0.1**	**0.1**	**0.2**	**0**	**0.4**	**0.7**	**0.1**	**0**	**0.2**	**0.1**	**0.2**	**0.2**	**0.1**	**0.2**	**0.3**
Average jitter (μsec)	**0.4**	**1.1**	**1**	**1.4**	**14**	**26**	**4.9**	**12**	**10**	**5.4**	**17**	**18**	**1.1**	**8.4**	**16**	**14**	**14**	**0.3**	**0.1**	**21**	**1.9**	**2.4**	**1.1**	**0.1**	**0.4**	**16**	**0.7**	**0.6**	**14**	**0.8**

Protocol

Table 2: Comparison of all routing protocols for 120 nodes.

Parameters	*OLSR*			*DSR*			*AODV*			*LAR1*			*DYMO*			*ZRP*			*STAR-LORA*			*STAR-ORA*			*Fisheye*			*Bellman–Ford*		
	CBR	FTP	VBR	CBR	FTP	VBR	CBR	FTP	VBR	CBR	FTP	VBR	CBR	FTP	VBR	CBR	FTP	VBR	CBR	FTP	VBR	CBR	FTP	VBR	CBR	FTP	VBR	CBR	FTP	VBR
Average transmission delay (μsec)	**28**	**49**	**39**	**24**	**42**	**36**	**18**	**27**	**33**	**27**	**50**	**43**	**31**	**55**	**41**	**29**	**38**	**49**	**26**	**48**	**54**	**31**	**36**	**44**	**26**	**46**	**48**	**33**	**32**	**44**
Receive power consumption (mWh)	**0.3**	**14**	**8**	**0.2**	**15**	**13**	**0.2**	**8.5**	**7**	**0.1**	**8.4**	**9**	**0.2**	**9**	**8.5**	**0.8**	**3**	**12**	**0.3**	**2.4**	**4**	**0.7**	**5**	**3**	**1.6**	**8.5**	**8**	**0.5**	**12**	**11**
Transmit power consumption (mWh)	**0.1**	**22**	**15**	**0.2**	**15**	**10**	**0.1**	**18**	**9**	**0.1**	**21**	**12**	**0.1**	**16**	**12**	**0.6**	**7**	**13**	**0.2**	**8**	**7**	**1.2**	**5**	**6.5**	**0.8**	**12**	**13**	**0.5**	**24**	**16**
Percentage of utilization	**0.8**	**1**	**1**	**0.8**	**0.8**	**0.3**	**0.3**	**0.3**	**0.6**	**0.6**	**0.3**	**0.4**	**0.7**	**0.7**	**0.8**	**0.1**	**0.4**	**0.4**	**0**	**0.7**	**0.7**	**0.1**	**0.2**	**0.6**	**0.1**	**0.4**	**0.5**	**0.1**	**0.3**	**0.5**
Average jitter (μsec)	**0.5**	**2.4**	**2**	**1.2**	**16**	**26**	**5.2**	**14**	**11**	**5.9**	**19**	**20**	**1.6**	**9.5**	**16**	**12**	**14**	**0.6**	**0.3**	**22**	**2.9**	**3.2**	**2.3**	**1.7**	**0.5**	**17**	**1.5**	**0.9**	**12**	**1.8**

Column group heading: *Protocol*

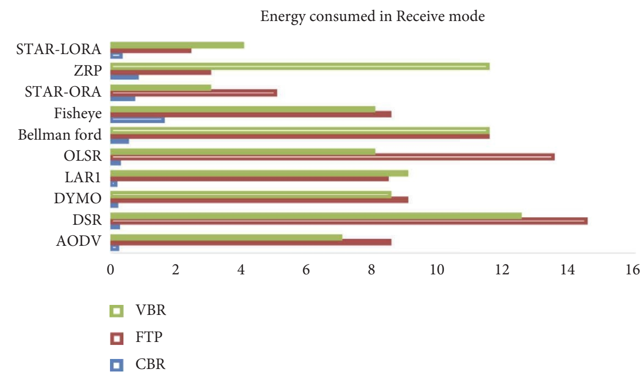

Figure 14: Receive mode energy consumption of all routing protocols for 60 nodes.

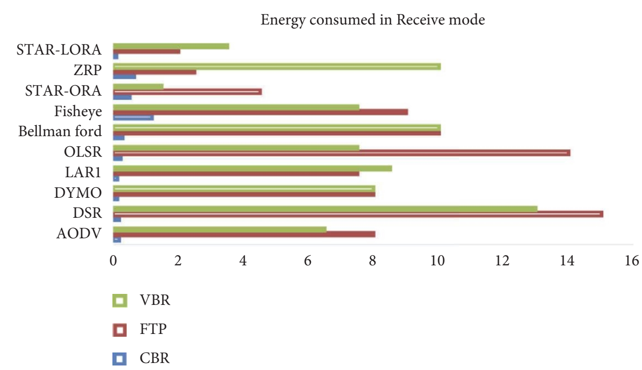

Figure 15: Receive mode energy consumption of all routing protocols for 120 nodes.

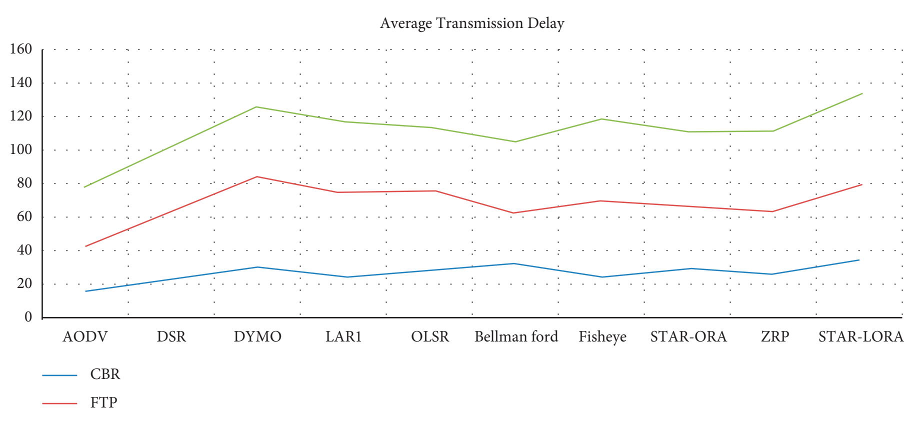

Figure 16: Average transmission delay of all routing protocols for 60 nodes.

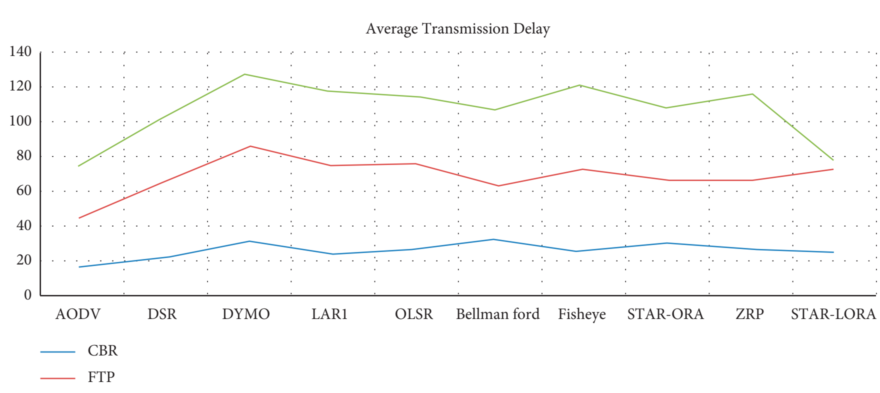

Figure 17: Average transmission delay of all routing protocols for 120 nodes.

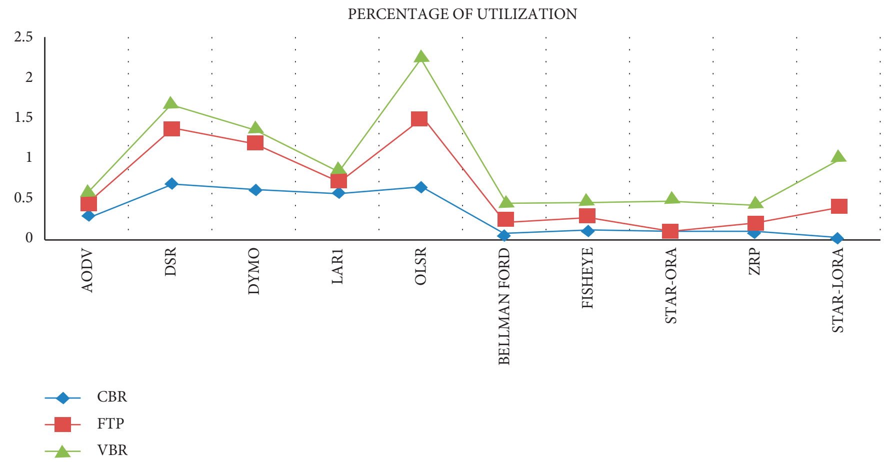

Figure 18: Percentage of utilisation of all routing protocols for 60 nodes.

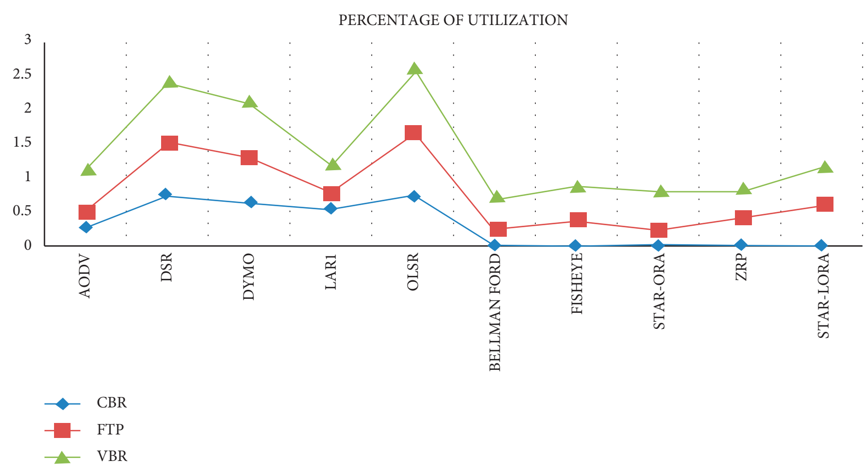

Figure 19: Percentage of utilisation of all routing protocols for 120 nodes.

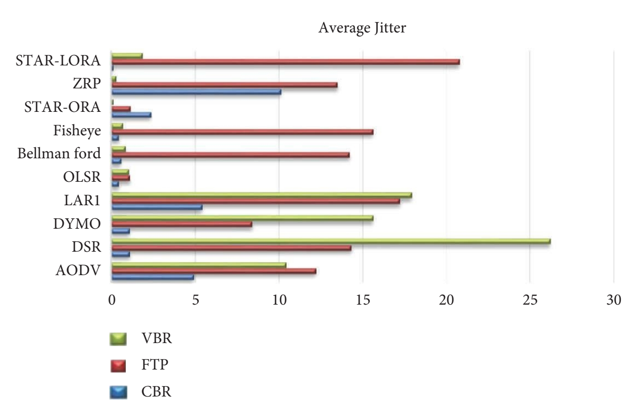

Figure 20: Average jitter of all routing protocols for 60 nodes.

(91.4%), and Figures 18 and 19 display the percentages of utilisation for the following routing protocols: AODV, DSR, DYMO, LAR1, Bellman–Ford, OLSR, fisheye, STAR-ORA, ZRP, and STAR-LORA.

4.5. Average Jitter (μsec) by AODV, DSR, DYMO, LAR1, Bellman–Ford, OLSR, Fisheye, STAR-ORA, ZRP, and STAR-LORA Routing Protocols. Each routing protocol has an average latency that is represented as jitter, as seen in

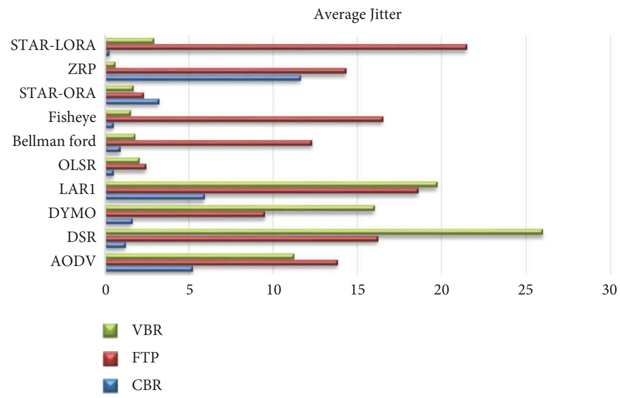

Figure 21: Average jitter of all routing protocols for 120 nodes.

Figures 20 and 21. As shown in Tables 1 and 2, STAR-LORA generates 85.3 percent less average jitter than the other routing protocols in the proposed network.

5. Conclusion

Along with the exploration of an underwater environment, other aspects are also evolving, such as the monitoring of underwater resources, the investigation of parameters, and the planning of military action. The extent of battery power is the primary focus of the network because the UWSN can only carry out certain tasks. This study compares the performance of the routing protocols AODV, DSR, DYMO, LAR1, Bellman–Ford, OLSR, fisheye, STAR-ORA, ZRP, and STAR-LORA in UWSN networks with variable deployment applications such as FTP, CBR, and VBR for 60 and 120 nodes, respectively. The metrics such as average transmission delay, average jitter, utilisation rate, and energy used in transmit and receive modes were all tracked. The simulation results show that when compared to the DSR, DYMO, LAR1, Bellman–Ford, OLSR, fisheye, STAR-ORA, ZRP, and STAR-LORA routing protocols, the AODV routing protocol generates the least overall energy with a slight variation of additional nodes as well as 88.6 percent less average transmission delay. In addition, compared to the AODV, DSR, DYMO, LAR1, Bellman–Ford, OLSR, fisheye, STAR-ORA, ZRP, and STAR-LORA routing protocols, the fisheye routing protocol achieves a 91.4 percent higher percentage of utilisation. The average jitter produced by STAR-LORA is 85.3 percent lower than that of the other routing protocols for 60 and 120 nodes.

Data Availability

The data used to support the findings of this study are available from the corresponding author upon request (head.research@bluecrest.edu.lr).

Conflicts of Interest

The authors declare that they have no conflicts of interest to report regarding the present study.

Authors' Contributions

K. Sathish conceptualized the study, performed data curation and formal analysis, proposed methodology, provided software, and wrote the original draft. C. V. Ravikumar supervised, visualized, and investigated the study and performed formal analysis. Asadi Srinivasulu applied a plagiarism checker and document remover. A. Rajesh visualized the study, proposed methodology, and edited and reviewed the manuscript. Olutayo Oyeyemi Oyerinde administered the project and acquired funding.

References

[1] M. Ayaz, I. Baig, A. Abdullah, and I. Faye, "A survey on routing techniques in underwater wireless sensor networks," *Journal of Network and Computer Applications*, vol. 34, no. 6, pp. 1908–1927, 2011.

[2] J. G. Proakis, E. M. Sozer, J. A. Rice, and M. Stojanovic, "Shallow water acoustic networks," *IEEE Communications Magazine*, vol. 39, no. 11, pp. 114–119, 2001.

[3] J. Heidemann, W. Ye, J. Wills, A. Syed, and Y. Li, "Research challenges and applications for underwater sensor networking," in *Proceedings of the Wireless Communications and Networking Conference (WCNC 2006)*, Las Vegas, NV, USA, April 2006.

[4] N. Meratnia, J. M. H. Paul, C. Paolo et al., "CLAM—collaborative embedded networks for submarine surveillance: an overview," in *Proceedings of the OCEANS, 2011 IEEE-Spain*, Santander, Spain, June 2011.

[5] S. Fang, L. D. Xu, Y. Zhu et al., "An integrated system for regional environmental monitoringand management based on internet of things," *IEEE Transactions on Industrial Informatics*, vol. 10, no. 2, pp. 1596–1605, 2014.

[6] E. M. Sozer, M. Stojanovic, and J. G. Proakis, "Underwater acoustic networks," *IEEE Journal of Oceanic Engineering*, vol. 25, no. 1, pp. 72–83, 2000.

[7] J. H. Cui, J. Kong, M. Gerla, and S. Zhou, "The challenges of building scalable mobile underwater wireless sensor networks for aquatic applications," *IEEE Network*, vol. 20, no. 3, pp. 12–18, 2006.

[8] S. Rani, S. H. Ahmed, J. Malhotra, and R. Talwar, "Energy efficient chain based routing protocol for underwater wireless

sensor networks," *Journal of Network and Computer Applications*, vol. 92, 2017.

[9] K. Wang, H. Gao, X. Xu, J. Jiang, and D. Yue, "An energy-efficient reliable data transmission scheme for complex environmental monitoring in underwater acoustic sensor networks," *IEEE Sensors Journal*, vol. 16, no. 11, pp. 4051–4062, 2016.

[10] G. Han, J. Jiang, L. Shu, and M. Guizani, "An attack-resistant trust model based on multidimensional trust metrics in underwater acoustic sensor network," *IEEE Transactions on Mobile Computing*, vol. 14, no. 12, pp. 2447–2459, 2015.

[11] G. Han, J. Jiang, L. Shu, Y. Xu, and F. Wang, "Localization algorithms of underwater wireless sensor networks: a survey," *Sensors*, vol. 12, no. 2, pp. 2026–2061, 2012.

[12] S. Lee and D. Kim, "Underwater hybrid routing protocol for UWSNs," in *Proceedings of the 5th International Conference on Ubiquitous and Future Networks (ICUFN)*, Da Nang, Vietnam, July 2013.

[13] F. Yuan, Y. Zhan, and Y. Wang, "Data density correlation degree clustering method for data aggregation in WSN," *IEEE Sensors Journal*, vol. 14, no. 4, pp. 1089–1098, 2014.

[14] R. Agarwal, S. Kumar, and R. M. Hegde, "Algorithms for crowd surveillance using passive acoustic sensors over a multimodal sensor network," *IEEE Sensors Journal*, vol. 15, no. 3, pp. 1920–1930, 2015.

[15] C. V. Ravikumar and P. B. Kala, "Design of MC-CDMA receiver using RBF network to mitigate MAI and nonlinear distortion," *Neural Computing & Applications*, vol. 31, 2019.

[16] C. Perkins, E. Belding-Royer, and S. Das, *Ad Hoc on-Demand Distance Vector (AODV) Routing. No. RFC 3561*, Internet Society, Reston, VA, USA, 2003.

[17] G. S. Teja and P. Samundiswary, "Performance analysis of DYMO protocol for IEEE 802.15. 4 based WSNs with mobile nodes," in *Proceedings of the Computer Communication and Informatics (ICCCI)*, Coimbatore, India, January 2014.

[18] M. K. Park and V. Rodoplu, "UWAN-MAC: an energy-efficient MAC protocol for underwater acoustic wireless sensor networks," *IEEE Journal of Oceanic Engineering*, vol. 32, no. 3, pp. 710–720, 2007.

[19] S. Rani, R. Talwar, J. Malhotra, S. H. Ahmed, M. Sarkar, and H. Song, "A novel scheme for an energy efficient internet of things based on wireless sensor networks," *Sensors*, vol. 15, no. 11, pp. 28603–28626, 2015.

[20] M. C. Domingo and R. Prior, "Energy analysis of routing protocols for underwater wireless sensor networks," *Computer Communications*, vol. 31, no. 6, pp. 1227–1238, 2008.

[21] C. V. Ravikumar and P. B. Kala, "MC-CDMA receiver design using recurrent neural network for eliminating MAI and non linear distortion," *International Journal of Communication Systems*, vol. 10, 2017.

[22] M. S. A. Patil and M. P. Mishra, "Improved mobicast routing protocol to minimize energy consumption for underwater wireless sensor networks," *International Journal of Research Science Engineering*, vol. 3, no. 2, pp. 197–204, 2017.

[23] A. Khan, I. Ahmedy, M. Anisi et al., "A localization-free interference and energy holes minimization routing for underwater wireless sensor networks," *Sensors*, vol. 18, no. 2, p. 165, 2018.

[24] S. H. Manjula, C. N. Abhilash, K. Shaila, K. R. Venugopal, and L. M. Patnaik, "Performance of AODV routing protocol using group and entity mobility models in wireless sensor networks," in *Proceedings of the International Multi Conference of Engineers and Computer Scientist*, Hong Kong, China, March 2008.

[25] K. Bhattacharjya, S. Alam, and D. De, "Performance analysis of DYMO, ZRP and AODV routing protocols in a multi hop grid based underwater wireless sensor network," in *Proceedings of the 2nd International Conference on Computational Intelligence, Communications and Business Analytics (CICBA)*, Kalyani, India, June 2018.

[26] K. Bhattacharjya, S. Alam, and D. De, "TTCBT: two tier complete binary tree based wireless sensor network for FSR and LANMAR routing protocols," *Microsystem Technologies*, vol. 27, no. 2, pp. 443–453, 2018.

[27] Z. Wang, G. Han, H. Qin, S. Zhang, and Y. Sui, "An energy-aware and void-avoidable routing protocol for underwater sensor networks," *IEEE Access*, vol. 6, pp. 7792–7801, 2018.

[28] Z. Alkindi, N. Alzeidi, and B. A. A. Touzene, "Performance evolution of grid based routing protocol for underwater wireless sensor networks under different mobile models," *International Journal of Wireless & Mobile Networks*, vol. 10, no. 1, pp. 13–25, 2018.

[29] R. Diamant and L. Lampe, "Underwater localization with time-synchronization and propagation speed uncertainties," *IEEE Transactions on Mobile Computing*, vol. 12, no. 7, pp. 1257–1269, 2013.

[30] P. K. Varshney, G. S. Agrawal, and S. K. Sharma, "Relative performance analysis of proactive routing protocols in wireless ad hoc networks using varying node density," *Invertis Journal of Science & Technology*, vol. 9, no. 3, pp. 161–169, 2016.

[31] K. Bhattacharjya, S. Alam, and D. C. De, "Energy efficient routing protocol selection for cluster-based underwater wireless sensor network," *Microsystem Technologies*, vol. 28, 2019.

[32] D. SahabulAlam, "Cloud smoke sensing model for AODV, RIP and STAR routing protocols using wireless sensor network in industrial township area," in *Proceedings of the Second International Conference on Research in Computational Intelligence and Communication Networks (ICRCICN)*, Kolkata, India, 2016.

[33] L. E. Emokpae, S. DiBenedetto, B. Potteiger, and M. Younis, "UREAL: underwater reflection enabled acoustic-based localization," *IEEE Sensors Journal*, vol. 14, no. 11, pp. 3915–3925, 2014.

[34] Q. Liang, B. Zhang, C. Zhao, and Y. Pi, "TDoA for passive localization: underwater versus terrestrial environment," *IEEE Transactions on Parallel and Distributed Systems*, vol. 24, no. 10, pp. 2100–2108, 2013.

[35] Z. Yu, C. Xiao, and G. Zhou, "Multi-objectivization-based localization of underwater sensors using magnetometers," *IEEE Sensors Journal*, vol. 14, no. 4, pp. 1099–1106, 2014.

[36] K. Sathish, C. V. Ravikumar, A. Srinivasulu, and A. K. Gupta, "Performance analysis of underwater wireless sensor network by deploying FTP, CBR, and VBR as applications," *Journal of Computer Networks and Communications*, vol. 2022, Article ID 7143707, 30 pages, 2022.

[37] Z. Fang, J. Wang, C. Jiang, X. Wang, and Y. Ren, "Average peak age of information in underwater information collection with sleep-scheduling," *IEEE Transactions on Vehicular Technology*, vol. 71, no. 9, pp. 10132–10136, 2022.

[38] Z. Fang, J. Wang, J. Du, X. Hou, Y. Ren, and Z. Han, "Stochastic optimization-aided energy-efficient information collection in internet of underwater things networks," *IEEE Internet of Things Journal*, vol. 9, no. 3, pp. 1775–1789, 2022.

[39] K. Bagadi, C. V. Ravikumar, K. Sathish et al., "Detection of signals in MC-CDMA using a novel iterative block decision feedback equalizer," *IEEE Access*, vol. 10, pp. 105674–105684, 2022.

[40] H. U. Yildiz, V. C. Gungor, and B. Tavli, "Packet size optimization for lifetime maximization in underwater acoustic sensor networks," *IEEE Transactions on Industrial Informatics*, vol. 15, no. 2, pp. 719–729, 2019.

[41] K. Sathish, C. V. Ravikumar, A. Rajesh, and G. Pau, "Underwater wireless sensor network performance analysis using diverse routing protocols," *Journal of Sensor and Actuator Networks*, vol. 11, no. 4, p. 64, 2022.